

Received March 15, 2020, accepted March 29, 2020, date of publication March 31, 2020, date of current version April 24, 2020.

Digital Object Identifier 10.1109/ACCESS.2020.2984728

Parameters Extraction of Photovoltaic Models Using Triple-Phase Teaching-Learning-Based Optimization

ZUOWEN LIAO¹, ZHIKUN CHEN², AND SHUIJIA LI³

¹College of Economics and Management, Beibu Gulf Big Data Resources Utilisation Laboratory, Beibu Gulf University, Qinzhou 535011, China

²Guangxi Key Laboratory of Marine Disaster in the Beibu Gulf, Beibu Gulf Big Data Resources Utilisation Laboratory, College of Resources and Environment, Beibu Gulf University, Qinzhou 535011, China

³Department of Computer Science, China University of Geosciences, Wuhan 430074, China

Corresponding author: Zhikun Chen (chzhikun@163.com)

This work was supported in part by the National Natural Science Foundation of China under Grant 41666003 and Grant 41966007, in part by the Qinzhou Scientific Research and Technology Development Plan Project under Grant 201714322, in part by the High-Level Talents Research Projects of Beibu Gulf University under Grant 2019KYQD27, and in part by the Construction Project of Characteristic Specialty and Experimental Training Teaching Base (Center) in Guangxi Undergraduate Universities.

ABSTRACT Parameters extraction of photovoltaic (PV) models is urgently desired for the simulation, control, and evaluation of PV systems. To accurately and reliably extract the parameters of different PV models, a triple-phase teaching-learning-based optimization (TPTLBO) is proposed in this paper. The novelty of TPTLBO lies in: i) teaching-learning-based optimization introduces a buffer phase and adopts a centroid strategy to update the position of intermediate learners, which further strengthens the exploration and exploitation; ii) the learners can select different phases and employ different learning strategies based on their knowledge level; iii) a dynamic control parameter replaces the original random parameter *rand* to enhance the search ability of algorithm. The parameters extraction performance of TPTLBO is verified through the single diode model, the double diode model, and three PV models. Experimental results demonstrate that TPTLBO achieves better performance in terms of accuracy and reliability compared to state-of-the-art algorithms.

INDEX TERMS Photovoltaic models, parameter extraction, teaching-learning-based optimization, triple-phase.

I. INTRODUCTION

In recent years, to deal with the environment pollution, global warming, and increasing energy shortage, many countries have been looked for renewable energy [1]. The research of several renewable sources, such as wind, wave, biomass, and so on, has attracted lots of attention [2]. Among the different available sources of renewable energy, solar energy is one of the most promising and potential alternatives due to its availability and cleanliness [3]. Solar energy can be converted into electricity through photovoltaic (PV) system, which has been extensively applied worldwide [4]. Since photovoltaic systems depend on weather and environmental factors, particularly temperature and global irradiance, the use of photovoltaic power is an important challenge [5]. Hence, in order

The associate editor coordinating the review of this manuscript and approving it for publication was Narsa T. Reddy.

to optimize or control a PV system, it is necessary to evaluate the actual behavior of PV arrays through accurate model based on measured current-voltage data [6]. The widely used models are the single diode and double diode models [7]. The accuracy of models parameters is important to the research of solar PV systems. Hence, it is essential to design efficient method to extract these model parameters.

Several attempts have been devoted to adopting deterministic methods for parameter extraction of PV models [8], [9]. However, these methods are highly dependent on the initial guess and sensitive to the characteristics of the objective function [10]. Besides, PV models are nonlinear and multi-modal problem, leading to poor solution when using deterministic methods.

To overcome the disadvantage of deterministic methods, meta-heuristic methods by natural phenomenon inspired have been considered as effective alternatives for parameter

extraction of PV models. Because they do not have strict requirements, thus can be easily implemented for real-world problems. Up to now, a great deal of meta-heuristic methods have been used to extract the parameters of PV models. They are genetic algorithm [11], particle swarm optimization [12], differential evolution [13]–[15], ant lion optimizer [16], simulated annealing algorithm [17], harmony search [7], artificial bee colony [18], flower pollination algorithm [19], biogeography-based optimization [20], JAYA algorithm [6], backtracking search algorithm [1], and other algorithms [21], [22]. Although these methods have demonstrated satisfactory results, it still needs further improvements in accuracy and reliability. Moreover, most meta-heuristic methods contain the control parameters that need to be given in advance. However, their optimal parameter settings are difficult and problem-dependent.

The teaching-learning-based optimization algorithm (TLBO) is a simple yet powerful heuristic method proposed by Rao for continuous non-linear large scale problems [23]. Recently, some TLBO variants have been developed to extract the PV parameters. In [24], an improved TLBO algorithm (LETLBO) with learning experience of other learners was presented to extract the parameters of PV models, and promising results were obtained. However, this method needs to balance the diversity and the mean solution of the population. In [25], authors employed generalized oppositional teaching-learning-based optimization to identify the PV parameters. Generalized opposition-based learning was combined with original TLBO through the initialization step and generation jumping to improve the convergence. A self-adaptive teaching-learning-based optimization (SATLBO) is applied in [26] for solar cell parameters. In SATLBO, different learners can select different learning phases based on their knowledge level. This self-adaptive strategy is able to efficiently enhance the performance of algorithm. In [10], a new hybrid teaching-learning-based artificial bee colony (TLABC) for the solar PV parameter estimation problems was proposed. To accurately and reliably identify the PV parameters, an improved teaching-learning-based optimization (ITLBO) algorithm is proposed [27]. In ITLBO, authors adopt different strategies in teaching and learning phase to balance exploration and exploitation. However, these TLBO variants also encounter the dilemma of insufficient accuracy and low reliability. In addition, although the above methods have solved the problems of exploration and exploitation to some extent, it still needs further study.

Based on the above considerations, in this paper, a triple-phase teaching-learning-based optimization (TPTLBO) is proposed to accurately and reliably identify the parameters of PV models. In TPTLBO, three improvements are proposed to deal with the shortcomings. First, basic TLBO introduces a buffer phase. In buffer phase, a centroid strategy is developed to modify the position of intermediate learner, which can further improve the ability between exploration and exploitation. Secondly, the learners can select different phases and adopt different learning strategies based on their knowledge level.

Finally, utilizing a dynamic parameter strategy instead of the random parameter (*rand*) can be advantageous for search ability of the algorithm. In this way, we can alleviate the trivial task to set the optimal parameter for different problems. To evaluate the performance of TPTLBO, the algorithm was employed to extract the parameters of different PV models, such as the single diode model (SDM), the double diode model (DDM), and the PV module models (SMM) that consist of a plurality of solar cells connected in series and/or in parallel. Experimental results show that our method can provide highly competitive results compared with other state-of-the-art methods.

The main contributions of this paper are as follows:

- A TPTLBO algorithm is proposed to extract the parameters of PV models. In TPTLBO, basic TLBO adds a buffer phase to further improve the ability to balance diversity and convergence. Moreover, learners can select different phases and employ different learning strategies according to their knowledge level.
- A dynamically controlling parameters method is proposed to improve the search capability of the algorithm.
- By comparing with other TLBO parameter estimation methods, TPTLBO demonstrates the accuracy and reliability in the experiments. Thus, it can be considered as an effective alternative to parameter extraction of PV models.

The rest of this paper is organized as follow. Section II introduces different PV models and the objective function. Section III describes the basic TLBO algorithm. The proposed TPTLBO is proposed in Section IV. The experimental results are shown and analyzed in Section V. Finally, Section VI concludes the paper.

II. PHOTOVOLTAIC MODELING AND PROBLEM FORMULATION

In the literature, there are two most commonly used mathematic models can explain the I - V characteristics of PV systems. In this section, brief mathematical descriptions of the single diode, the double diode model, and the PV module are introduced.

A. SINGLE DIODE MODEL

Fig. 1(a) shows the equivalent circuit diagram for single diode model. It contains a current source, a diode, a shunt resistor and a series resistor. The output current is computed as follows:

$$I = I_{ph} - I_d - I_{sh} \quad (1)$$

where I_{ph} is the photo-generated current, I_d is the diode current, and I_{sh} represents the shunt resistor current. Among them, I_d and I_{sh} can be calculated as:

$$I_d = I_o \left[\exp \left(\frac{V + IR_s}{aV_t} \right) - 1 \right] \quad (2)$$

$$I_{sh} = \frac{V + IR_s}{R_{sh}} \quad (3)$$

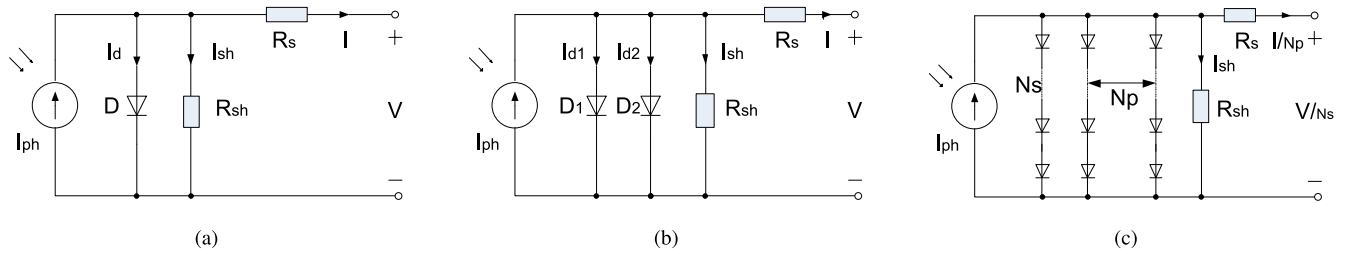


FIGURE 1. Equivalent circuit of PV models [27]: (a) SDM, (b) DDM, (c) SMM.

where I_o denotes the diode reverse saturation current, a is the diode ideality factor, R_s and R_{sh} are series and shunt resistance, respectively. V is the cell output voltage, and V_t represents the junction thermal voltage calculated by (4)

$$V_t = \frac{k \cdot T}{q} \quad (4)$$

where k is the Boltzmann constant ($1.3806503 \times 10^{-23}$ J/K), q is the electron charge ($1.60217646 \times 10^{-19}$ C), and T is the temperature of junction in Kelvin.

Therefore, according to (1)-(4), the output current I can be calculated by (5)

$$I = I_{ph} - I_o \left[\exp \left(\frac{V + IR_s}{aV_t} \right) - 1 \right] - \frac{V + IR_s}{R_{sh}} \quad (5)$$

Therefore, there are five unknown parameter (I_{ph} , I_o , R_s , R_{sh} , and a) that require to be identified in single diode model.

B. DOUBLE DIODE MODEL

For the double diode model, Fig. 1(b) shows that two diodes in parallel in the equivalent circuit. The output current I is calculated as follows:

$$I = I_{ph} - I_{d1} - I_{d2} - I_{sh} \quad (6)$$

where I_{d1} , I_{d2} are respectively the first and second diode currents, which can be computed as below:

$$I_{d1} = I_{o1} \left[\exp \left(\frac{V + IR_s}{a_1 V_t} \right) - 1 \right] \quad (7)$$

$$I_{d2} = I_{o2} \left[\exp \left(\frac{V + IR_s}{a_2 V_t} \right) - 1 \right] \quad (8)$$

where I_{o1} , I_{o2} represent diffusion current and saturation current, respectively. a_1 , a_2 denote the first and second diode ideality factors, respectively. Therefore, the output current I of solar cell can be calculated by (9), and DDM has seven unknown parameters (I_{ph} , I_{o1} , I_{o2} , R_s , R_{sh} , a_1 , and a_2) that need to be extracted:

$$I = I_{ph} - I_{o1} \left[\exp \left(\frac{V + IR_s}{a_1 V_t} \right) - 1 \right] - I_{o2} \left[\exp \left(\frac{V + IR_s}{a_2 V_t} \right) - 1 \right] - \frac{V + IR_s}{R_{sh}} \quad (9)$$

C. PHOTOVOLTAIC MODULE MODEL

Fig. 1(c) demonstrates the equivalent circuit of the PV module. It can be observed that the PV module consist of several diodes connected in series and/or in parallel. The output current is calculated as follows:

$$I = I_{ph} N_p - I_o N_p \left[\exp \left(\frac{V + IR_s N_s / N_p}{a N_s V_t} \right) - 1 \right] - \frac{V + IR_s N_s / N_p}{R_{sh} N_s / N_p} \quad (10)$$

where N_s and N_p are the number of solar cells connected in series or in parallel, respectively. Because PV models used in this paper are all in series, N_p is equal to 1. It is observed that five parameters (I_{ph} , I_o , R_s , R_{sh} , and a) require to be extracted.

D. OBJECTIVE FUNCTION

In general, the problem of PV parameter extraction can be converted into an optimization problem, and the goal is to minimize the error between the experimental data and simulated data. The overall error between measured and calculated current data is defined as follows:

$$RMSE(\mathbf{x}) = \sqrt{\frac{1}{N} \sum_{k=1}^N f(V_k, I_k, \mathbf{x})^2} \quad (11)$$

where N is the number of experimental data, and \mathbf{x} is a vector that contains the parameters to be identified. In this paper, the objective functions of different PV models can be calculated as follow:

- For SDM:

$$\begin{cases} f(V, I, \mathbf{x}) = I_{ph} - I_o \left[\exp \left(\frac{V + IR_s}{aV_t} \right) - 1 \right] \\ - \frac{V + IR_s}{R_{sh}} - I \\ \mathbf{x} = \{I_{ph}, I_o, R_s, R_{sh}, a\} \end{cases} \quad (12)$$

- For DDM:

$$\begin{cases} f(V, I, \mathbf{x}) = I_{ph} - I_{o1} \left[\exp \left(\frac{V + IR_s}{a_1 V_t} \right) - 1 \right] \\ - I_{o2} \left[\exp \left(\frac{V + IR_s}{a_2 V_t} \right) - 1 \right] - \frac{V + IR_s}{R_{sh}} - I \\ \mathbf{x} = \{I_{ph}, I_{o1}, I_{o2}, R_s, R_{sh}, a_1, a_2\} \end{cases} \quad (13)$$

- For SMM:

$$\begin{cases} f(V, I, \mathbf{x}) = I_{ph} - I_o \left[\exp\left(\frac{V + IR_s N_s}{a N_s V_t}\right) - 1 \right] \\ - \frac{V + IR_s N_s}{R_{sh} N_s} - I \\ \mathbf{x} = \{I_{ph}, I_o, R_s, R_{sh}, a\} \end{cases} \quad (14)$$

III. TEACHING-LEARNING-BASED OPTIMIZATION

Inspired by the interaction between teachers and students in class, TLBO was first proposed to deal with nonlinear optimization problems [28]. The main idea of TLBO is to mimic the classical learning process composed of a teacher phase and a learner phase. In the teacher phase, teacher shares his/her knowledge to enhance the mean of the class; whereas in the learner phase, learners can communicate with each other to improve their knowledge level. These two phases will be introduced in the subsequent sections.

A. TEACHER PHASE

Generally, a class consists of one teacher and $NP - 1$ learners ($\mathbf{x}_i, i = 1, \dots, NP$). The best learner is considered as the teacher ($\mathbf{x}_{teacher}$) and he/she can share the knowledge to the learners to enhance the mean of the class. The mean position of a class can be defined as:

$$\mathbf{x}_{mean} = \frac{1}{NP} \sum_{i=1}^{NP} \mathbf{x}_i \quad (15)$$

subsequently, each learner is updated as follows:

$$\mathbf{x}_{i,new} = \mathbf{x}_i + rand \cdot (\mathbf{x}_{teacher} - T_F \cdot \mathbf{x}_{mean}) \quad (16)$$

where $\mathbf{x}_{i,new}$ and \mathbf{x}_i represent the i -th learner's new and old positions. $rand$ is the random number between 0 and 1. T_F is the teaching factor and its value is equal to either 1 or 2.

B. LEARNER PHASE

In the learner phase, a learner selects different learners and interacts randomly with them to improve his/her knowledge level. The learning process can be formulated as follows:

$$\mathbf{x}_{i,new} = \begin{cases} \mathbf{x}_i + rand \cdot (\mathbf{x}_i - \mathbf{x}_j), & \text{if } f(\mathbf{x}_i) \leq f(\mathbf{x}_j) \\ \mathbf{x}_i + rand \cdot (\mathbf{x}_j - \mathbf{x}_i), & \text{otherwise} \end{cases} \quad (17)$$

where \mathbf{x}_j is j -th learner and $i \neq j$. $f(\mathbf{x})$ is the fitness value of \mathbf{x} .

IV. OUR APPROACH: TPTLBO

A. MOTIVATIONS

In the original TLBO algorithm, learners require to undergo the teacher phase and learner phase, which results in the consumption of more fitness evaluations in each generation [29]. Moreover, to balance between exploration and exploitation, several researchers have proposed improved methods, such as LETLBO [24], GOTLBO [25], SATLBO [26], TLABC [10], ITLBO [27]. However, the balance ability needs further

improvement. In addition, as shown in (16) and (17), a random number ($rand$) is used to scale the difference between learners, which will affect the performance of TLBO. For example, if $rand$ is small in the early stage, it is not conducive to global search and population diversity; whereas at a later stage, a larger $rand$ may lead to a slow convergence. Hence, its optimal parameter setting is difficult and problem-dependent.

In this paper, we present a triple-phase TLBO for parameter extraction of different PV models. It is explained in detail in the subsequent subsections.

B. TEACHER PHASE OF TPTLBO

In the teacher phase of TPTLBO, we adopt the strategy proposed in [27] to improve the convergence rate. Thus, the modification of learner in teacher phase is described as:

$$\mathbf{x}_{i,new} = \mathbf{x}_i + F_t \cdot (\mathbf{x}_{teacher} - \mathbf{x}_i) + F_t \cdot (\mathbf{x}_{r1} - \mathbf{x}_{r2}) \quad (18)$$

where r_1, r_2 are random integers selected from $\{1, \dots, NP\}$ and $r_1 \neq r_2 \neq i$. F_t is a dynamic control parameter, which will be introduced in Section IV-F.

The teaching strategy offers two exclusive advantages. On the one hand, better learners can approach the promising region by the teacher ($\mathbf{x}_{teacher}$) and themselves (\mathbf{x}_i). On the other hand, By increasing the disturbance of different learners, it avoids falling into local optima.

C. LEARNER PHASE OF TPTLBO

In the learner phase, the exploration ability plays a vital role in refining the quality of learners. However, The strategy used in the learning phase of the original TLBO results in limited learner capability and fewer global searching, making it difficult to maintain population diversity. Hence, in [26], authors introduced a diversity learning method to improve the exploration ability of the algorithm. In TPTLBO, we adopt this method directly to update the learner's position, which is described as follows:

$$\mathbf{x}_{i,new} = \begin{cases} \mathbf{x}_i + F_t \cdot (\mathbf{x}_{r1} - \mathbf{x}_{r2}), & \text{if } f(\mathbf{x}_{r1}) \leq f(\mathbf{x}_{r2}) \\ \mathbf{x}_i + F_t \cdot (\mathbf{x}_{r2} - \mathbf{x}_{r1}), & \text{otherwise} \end{cases} \quad (19)$$

where r_1, r_2 are random integers selected from $\{1, \dots, NP\}$ and $r_1 \neq r_2 \neq i$. F_t is a dynamic control parameter.

D. BUFFER PHASE OF TPTLBO

For better learners and worse learners, it is easy to choose appropriate strategies to enhance the performance of the algorithm according to their characteristics. However, for intermediate learners, their preference is not obvious. Therefore, it is inappropriate to choose the teaching or learning phase strategy to update the position. To this end, we introduce the buffering phase in the original TLBO and use the centroid strategy to update the learner's position. The centroid strategy was first proposed in [30]. In this paper, we make a minor

modify for brevity.

$$\mathbf{x}_{i,new} = \mathbf{x}_{mean} + F_t \cdot (\mathbf{x}_{r1} - \mathbf{x}_{r2}) \quad (20)$$

As shown in (15), the mean position (\mathbf{x}_{mean}) is calculated based on the position of each learner. Hence, only the partial information of each learner is inherited by the mean learner. According to (20), previously explored areas can be fully exploited, while other potential areas can also be explored [30]. Therefore, the use of centroid strategy by intermediate learners can further balance the performance of exploration and exploitation.

E. SELF-ADAPTIVELY SELECT THE LEARNING PHASE

First, all learners are sorted in ascending order (from the best to the worst) based on their fitness. According to the ranking, learners can be divided into three categories: better learners, intermediate learners, and worse learners. The ranking formula is as follows:

$$\mathbf{x}_i = \begin{cases} \text{better learners,} & \text{if } i \in (1, \lfloor NP/3 \rfloor) \\ \text{intermediate learners,} & \text{if } i \in (\lfloor NP/3 \rfloor + 1, \lfloor 2NP/3 \rfloor) \\ \text{worse learners,} & \text{otherwise} \end{cases} \quad (21)$$

Algorithm 1 Self-Adaptively Select the Learning Phase

```

1 Sort the population in ascending order according to the fitness;
2 for i = 1 to NP do
3   if i ∈ (1, ⌊NP/3⌋) then
4     Implement the teacher phase of TPTLBO;
5     else if i ∈ (⌊NP/3⌋ + 1, ⌊2NP/3⌋) then
6       Implement the buffer phase of TPTLBO;
7     else
8       Implement the learner phase of TPTLBO;
9     end
10  end
11 end
12 end
    
```

Based on the aforementioned classification, the learners can select the appropriate learning phases adaptively. Algorithm 1 describes the selection process. For the better learners, teacher phase will be chosen to improve the convergence ability, while the worse learners are chosen learner phase to enhance the population diversity. In addition, intermediate learners will choose buffer phase to further improve

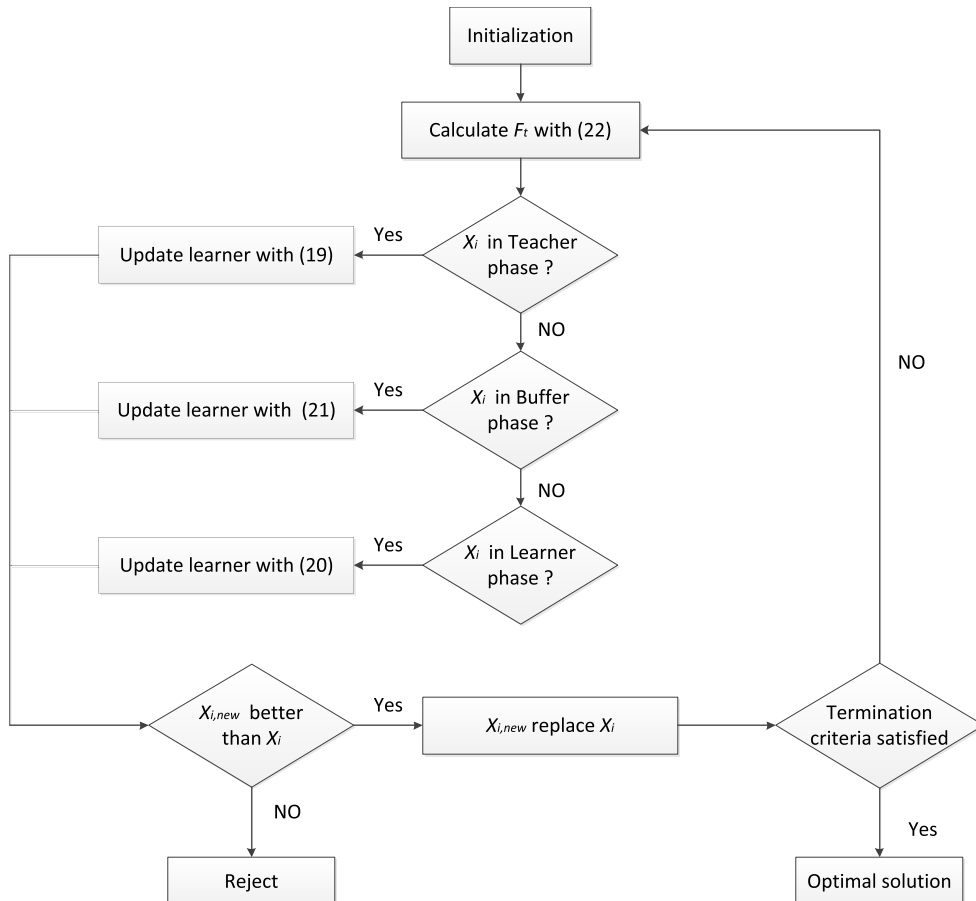


FIGURE 2. Flow chart of the TPTLBO.

the balance between exploration and exploitation. Hence, under the same number of fitness evaluations, self-adaptive selection strategy can search efficiently and enhance the performance of TLBO.

F. DYNAMIC CONTROL TECHNIQUE

As shown in (16) and (17), a random parameter (*rand*) is used to control the amount of knowledge acquired from other learners. It has some disadvantages. For example, too small *rand* value in the early stage may lead to less knowledge from other learners, which is not conducive to the exploration performance of the algorithm. In contrast, too large *rand* at the later stage may result in reducing the exploitation ability of the algorithm. In this section, we introduce a dynamic control technique [31] to deal with the problem.

$$F_t = F_{\min} + \lambda_t \times (F_{\max} - F_{\min}) \tag{22}$$

where F_t is the current control parameter at iteration t ; F_{\min} and F_{\max} are the minimal and maximal values of the control parameter; $F_{\min} = 0.5, F_{\max} = 0.9^1$; and $\lambda_t \in [0, 1]$ is dynamically changed during the run. λ_t is calculated as follows:

$$\lambda_t = 1 - \frac{NFE}{NFE_{\max}} \tag{23}$$

where NFE is the current numbers of fitness evaluation; and NFE_{\max} is the maximal NFE . It can be seen clearly that λ_t gradually decreases from 1 to 0 during the run. The reason is that:

- In the early stage, a large F_t can ensure that more knowledge can be obtained from other learners, which is in favor of exploration and population diversity.
- In the later stage, the algorithm has explored several promising areas. A small F_t is beneficial to improve the exploitation ability and obtain high-quality solution.

G. FRAMEWORK OF TPTLBO

The pseudo-code of TPTLBO is described in Algorithm 2, where NP is the population size, NFE is the current number of fitness evaluation, and NFE_{\max} is the maximal NFE . Besides, the flow chart of TPTLBO is given in Fig. 2.

TPTLBO has the following merits: (1) it adds a buffer phase to the original TLBO to further balance the ability between exploration and exploitation; (2) a centroid strategy is used to update the position of the learner in the buffer phase; (3) a method for dynamically controlling parameter is introduced to enhance the search efficiency. Algorithm 2 demonstrates that TPTLBO is also simple. The complexity of TPTLBO does not increase compared with that of TLBO.

¹We did a lot of experiments and verified that $F_{\min} = 0.5, F_{\max} = 0.9$ obtained better results in the parameter extraction of different models. Therefore, this paper adopts these two parameter values.

Algorithm 2 The Framework of TPTLBO

```

Input: Control parameters:  $NP, NFE, NFE_{\max}$ 
Output: The optimal solution
1 Set  $NFE = 0, Iter = 1$ ;
2 Randomly generate the population ;
3 Evaluate the fitness of the population ;
4  $NFE = NFE + NP$ ;
5 while  $NFE < NFE_{\max}$  do
6   Calculate  $F_t$  via (22);
7   Rank and classify learners according to their fitness;
8   for  $i = 1$  to  $NP$  do
9     if  $i \in (1, \lfloor NP/3 \rfloor)$  then // Teacher phase
10      Calculate  $x_{i,new}$  via (18)
11    end
12    else if  $i \in (\lfloor NP/3 \rfloor + 1, \lfloor 2NP/3 \rfloor)$  then
13      // Buffer phase
14      Calculate  $x_{i,new}$  via (20)
15    end
16    else // Learner phase
17      Calculate  $x_{i,new}$  via (19)
18    end
19  end
20  if  $f(x_{i,new}) \leq f(x_i)$  then
21     $x_i = x_{i,new}$ ;
22  end
23  $NFE = NFE + NP$ ;
24 return the best individual from the final population.

```

TABLE 1. Parameter settings of different algorithms.

Algorithm	Parameter setting
IJAYA	$NP = 20$
PGJAYA	$NP = 20$
MLBSA	$NP = 50$
TLBO	$NP = 50$
SATLBO	$NP = 40$
LETLBO	$NP = 50$
GOTLBO	$NP = 50$, jumping rate $J_r = 0.3$
TLABC	$NP = 50$, $limit = 200$, scale factor $F = rand(0, 1)$
ITLBO	$NP = 50$
TPTLBO	$NP = 50$
CPMPSO	$NP = 50, w = 0.729, c_1 = 1.49445, c_2 = 1.49445$
BLPSO	$NP = 40, w = 0.9 \sim 0.2, c = 1.496, I = E = 1$
FPA	$NP = 25, P = 0.8$
GWO	$NP = 30, a = 2 \sim 0$
WDO	$NP = 20, RT = 3, g = 0.2, \alpha = 0.4, c = 0.4$

V. RESULTS AND ANALYSIS

To evaluate the performance of TPTLBO, the algorithm is used to extract the parameters of different PV models: the single diode model, double diode model, and PV module models.

- For the single and double diode models, their current-voltage data was received from [8], which is measured on a 57 mm diameter commercial silicon R.T.C France solar cell (under $1000 W/m^2$ at $33^\circ C$).
- The PV models include three different modules: poly-crystalline Photowatt-PWP201, mono-crystalline

TABLE 2. Parameter ranges of different PV models.

Parameter	SDM/DDM		Photowatt-PWP201		STM6-40/36		STP6-120/36	
	LB	UB	LB	UB	LB	UB	LB	UB
I_{ph} (A)	0	1	0	2	0	2	0	8
I_o, I_{o1}, I_{o2} (μ A)	0	1	0	50	0	50	0	50
R_s (Ω)	0	0.5	0	2	0	0.36	0	0.36
R_{sh} (Ω)	0	100	0	2000	0	1000	0	1500
a, a_1, a_2	1	2	1	50	1	60	1	50

TABLE 3. Comparison of TPTLBO with other algorithms on the single diode model.

Algorithm	I_{ph} (A)	I_d (μ A)	R_s (Ω)	R_{sh} (Ω)	a	RMSE
IJAYA	0.7608	0.3281	0.0364	53.7595	1.4811	9.8603E-04
PGJAYA	0.7608	0.3230	0.0364	53.7185	1.4812	9.8602E-04
MLBSA	0.7608	0.3230	0.0364	53.7185	1.4812	9.8602E-04
TLBO	0.7607	0.3294	0.0363	54.3015	1.4831	9.8733E-04
SATLBO	0.7608	0.3232	0.0364	53.7256	1.4812	9.8602E-04
LETLBO	0.7608	0.3222	0.0364	53.6655	1.4809	9.8603E-04
GOTLBO	0.7608	0.3226	0.0364	53.3388	1.4811	9.8658E-04
TLABC	0.7608	0.3230	0.0364	53.7164	1.4812	9.8602E-04
ITLBO	0.7608	0.3230	0.0364	53.7185	1.4812	9.8602E-04
TPTLBO	0.7608	0.3230	0.0364	53.7185	1.4812	9.8602E-04

STM6-40/36, and poly-crystalline STP6-120/36. The Photowatt-PWP201 has 36 cell joined together in series and is obtained under $1000 W/m^2$ at $45^\circ C$ [8]. The STM6-40/36 and STP6-120/36 both consist of 36 cells connected in series and are measured at $51^\circ C$ and $55^\circ C$. Their current-voltage data was gained from [32].

In this paper, nine well-established algorithms, such as IJAYA [6], PGJAYA [33], MLBSA [34], TLBO [23], LETLBO [24], GOTLBO [25], SATLBO [26], TLABC [10],

ITLBO [27], are compared with TPTLBO. Table 1 gives the parameter settings of the compared algorithm. All algorithms were executed in Matlab2013b software and each algorithm is carried out 30 independent runs. The experiments are performed on a desktop PC with Intel Core i7-7700 processor @ 3.6GHz, 8GB RAM, under the windows 10 64-bit OS.

For fair comparison, the ranges for each parameter are presented in Table 2, which are the same as used in the compared algorithms.

A. RESULTS ON THE SINGLE DIODE MODEL

For the single diode model, the results of the parameters extracted by different algorithms are shown in Table 3, where the best results are highlighted in **boldface**.

From Table 3, it can be seen that TPTLBO, ITLBO, TLABC, SATLBO, MLBSA, and PGJAYA provided the best RMSE values (**9.8602E-04**) followed by LETLBO, IJAYA, GOTLBO, and TLBO. Although the RMSE values obtained

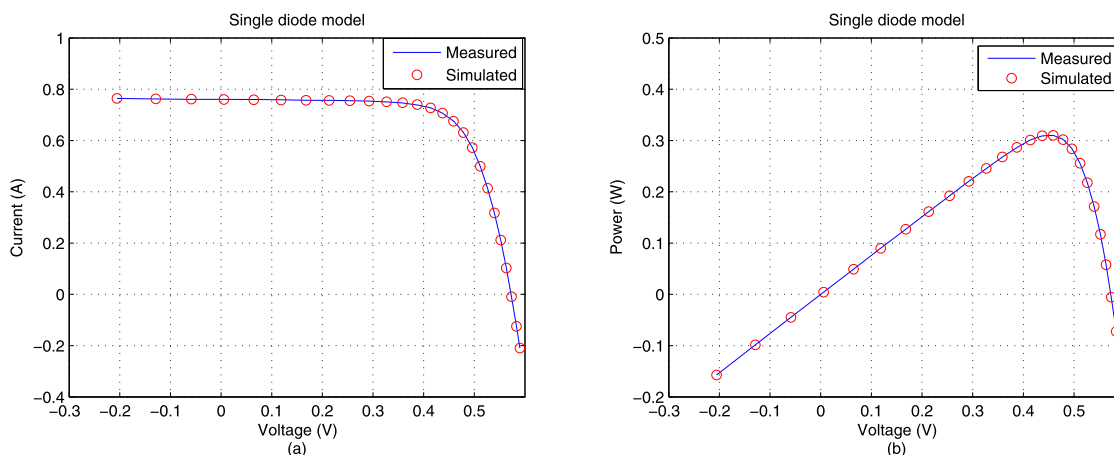


FIGURE 3. Comparison between the measured and simulated data obtained by TPTLBO for the single diode model: (a) *I-V* characteristic, (b) *P-V* characteristic.

TABLE 4. Comparison of TPTLBO with other algorithms on the double diode model.

Algorithm	I_{ph} (A)	I_{d1} (μ A)	R_s (Ω)	R_{sh} (Ω)	a_1	I_{d2} (μ A)	a_2	RMSE
IJAYA	0.7601	0.0050	0.0376	77.8519	1.2186	0.7509	1.6247	9.8293E-04
PGJAYA	0.7608	0.2103	0.0368	55.8135	1.4450	0.8853	2.0000	9.8263E-04
MLBSA	0.7608	0.2273	0.0367	55.4612	1.4515	0.7384	2.0000	9.8249E-04
TLBO	0.7610	0.2947	0.0366	53.1210	1.4730	0.1373	1.9938	1.0069E-03
SATLBO	0.7608	0.2509	0.0366	55.1170	1.4598	0.5454	1.9994	9.8280E-04
LETLBO	0.7608	0.1137	0.0364	54.0688	1.9284	0.3032	1.4760	9.8571E-04
GOTLBO	0.7608	0.2717	0.0366	53.6187	1.4668	0.2595	1.9161	9.9544E-04
TLABC	0.7608	0.4239	0.0367	54.6680	1.9075	0.2401	1.4567	9.8415E-04
ITLBO	0.7608	0.2260	0.0367	55.4854	1.4510	0.7493	2.0000	9.8248E-04
TPTLBO	0.7608	0.7434	0.0367	55.4831	2.0000	0.2266	1.4513	9.8248E-04

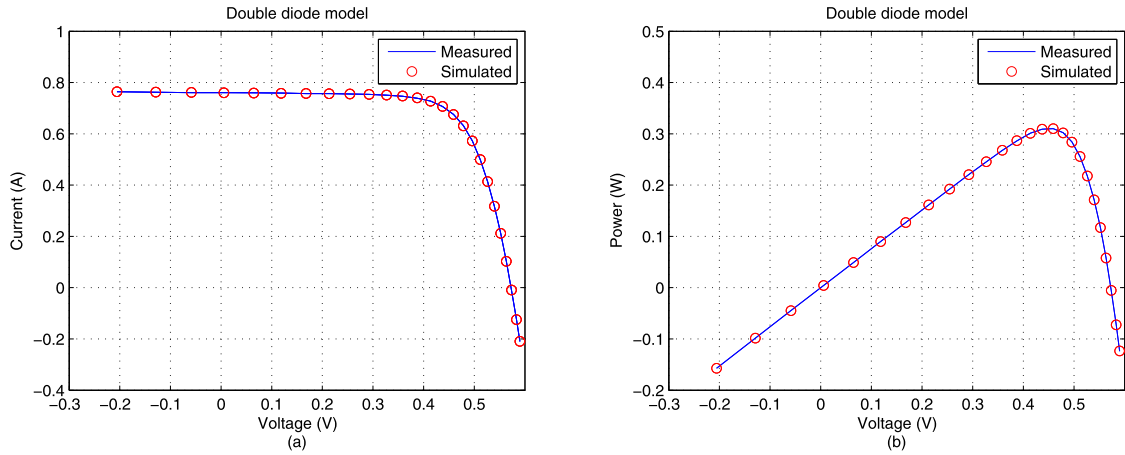


FIGURE 4. Comparison between the measured and simulated data obtained by TPTLBO for the double diode model: (a) I - V characteristic, (b) P - V characteristic.

TABLE 5. Simulated results of TPTLBO for double diode model.

Item	V (V)	$I_{measured}$ (A)	$I_{simulated}$ (A)	IAEC (A)
1	-0.2057	0.764	0.764041	0.000040546
2	-0.1291	0.762	0.762636	0.000636046
3	-0.0588	0.7605	0.761347	0.000846863
4	0.0057	0.7605	0.760163	0.00033673
5	0.0646	0.76	0.75908	0.000920348
6	0.1185	0.759	0.758079	0.000921215
7	0.1678	0.757	0.757135	0.000135348
8	0.2132	0.757	0.756188	0.000811971
9	0.2545	0.7555	0.755128	0.000372329
10	0.2924	0.754	0.75369	0.000309933
11	0.3269	0.7505	0.751391	0.000890646
12	0.3585	0.7465	0.747324	0.000823624
13	0.3873	0.7385	0.740048	0.001548263
14	0.4137	0.728	0.727337	0.000663244
15	0.4373	0.7065	0.7069	0.000400476
16	0.459	0.6755	0.675267	0.000233442
17	0.4784	0.632	0.630887	0.001112902
18	0.496	0.573	0.57211	0.000890403
19	0.5119	0.499	0.499528	0.000528143
20	0.5265	0.413	4.14E-01	0.000522166
21	0.5398	0.3165	0.317229	0.000729384
22	0.5521	0.212	0.212093	0.000092673
23	0.5633	0.1035	0.102698	0.000801930
24	0.5736	-0.01	-0.00927	0.000728759
25	0.5833	-0.123	-0.12439	0.001385340
26	0.59	-0.21	-0.20917	0.000828562
Σ	-	-	-	0.017511287

from are very close to the best RMSE value, it is significant for any reduction in the objective function. Since the exact parameter values were unavailable, the smaller the value of RMSE, the more accurate the extracted parameter.

In addition, to further confirm the accuracy of the extracted parameters, Fig. 3 plots the I - V and P - V curves. It is obvious that the simulated data from TPTLBO are highly matched with the measured data in the voltage range for both the I - V and P - V curves.

B. RESULTS ON THE DOUBLE DIODE MODEL

In the double diode model, there are seven unknown parameters. More parameters increase the difficulty of extracting parameters with the optimization algorithm. The extracted results of these algorithms are shown in Table 4. According

TABLE 6. Comparison of TPTLBO with other algorithms on the Photowatt-PWP201 module.

Algorithm	I_{ph} (A)	I_d (μ A)	R_s (Ω)	R_{sh} (Ω)	α	RMSE
IJAYA	1.0302	3.4703	1.2016	977.3752	48.6298	2.4251E-03
PGJAYA	1.0305	3.4818	1.2013	981.8545	48.6424	2.4251E-03
MLBSA	1.0305	3.4823	1.2013	981.9823	48.6428	2.4251E-03
TLBO	1.0305	3.4872	1.2011	984.8760	48.6482	2.4251E-03
SATLBO	1.0305	3.4827	1.2013	982.4038	48.6433	2.4251E-03
LETLBO	1.0305	3.4709	1.2017	981.0293	48.6302	2.4251E-03
GOTLBO	1.0305	3.4991	1.2008	989.6889	48.6611	2.4251E-03
TLABC	1.0306	3.4715	1.2017	972.9357	48.6313	2.4251E-03
ITLBO	1.0305	3.4823	1.2013	981.9823	48.6428	2.4251E-03
TPTLBO	1.0305	3.4823	1.2013	981.9822	48.6428	2.4251E-03

TABLE 7. Comparison of TPTLBO with other algorithms on the STM6-40/36 module.

Algorithm	I_{ph} (A)	I_d (μ A)	R_s (Ω)	R_{sh} (Ω)	α	RMSE
IJAYA	1.6637	1.8353	0.0040	15.9449	1.5263	1.7548E-03
PGJAYA	1.6639	1.7389	0.0043	15.9290	1.5203	1.7298E-03
MLBSA	1.6639	1.7387	0.0043	15.9283	1.5203	1.7298E-03
TLBO	1.6638	1.7307	0.0043	15.9955	1.5198	1.7305E-03
SATLBO	1.6639	1.7387	0.0043	15.9283	1.5203	1.7298E-03
LETLBO	1.6639	1.7387	0.0043	15.9283	1.5203	1.7298E-03
GOTLBO	1.6639	1.7387	0.0043	15.9283	1.5203	1.7298E-03
TLABC	1.6639	1.7387	0.0043	15.9283	1.5203	1.7298E-03
ITLBO	1.6639	1.7387	0.0043	15.9283	1.5203	1.7298E-03
TPTLBO	1.6639	1.7387	0.0043	15.9283	1.5203	1.7298E-03

TABLE 8. Comparison of TPTLBO with other algorithms on the STP6-120/36 module.

Algorithm	I_{ph} (A)	I_d (μ A)	R_s (Ω)	R_{sh} (Ω)	α	RMSE
IJAYA	7.4672	2.2536	0.0046	27.5925	1.2571	1.6731E-02
PGJAYA	7.4725	0.0000	0.0046	22.2184	1.2601	1.6601E-02
MLBSA	7.4725	2.3350	0.0046	22.2199	1.2601	1.6601E-02
TLBO	7.4782	1.9194	0.0047	13.2688	1.2440	1.6892E-02
SATLBO	7.4725	2.3350	0.0046	22.2199	1.2601	1.6601E-02
LETLBO	7.4725	2.3350	0.0046	22.2199	1.2601	1.6601E-02
GOTLBO	7.4725	2.3350	0.0046	22.2199	1.2601	1.6601E-02
TLABC	7.4725	2.3349	0.0046	22.2117	1.2601	1.6601E-02
ITLBO	7.4725	2.3350	0.0046	22.2199	1.2601	1.6601E-02
TPTLBO	7.4725	2.3350	0.0046	22.2199	1.2601	1.6601E-02

to the RMSE results, TPTLBO and ITLBO shown the best results among the nine algorithms.

The extracted TPTLBO parameter were used to plot I - V and P - V characteristics given as Fig. 4. It can be seen that the extracted data obtained by TPTLBO are highly fitted with the measured data. Additionally, the IAEC² is given in Table 5. IAEC describes the error between the extracted parameter

²Absolute error between measured and simulated power is calculated as $|I_{measured} - I_{simulated}|$

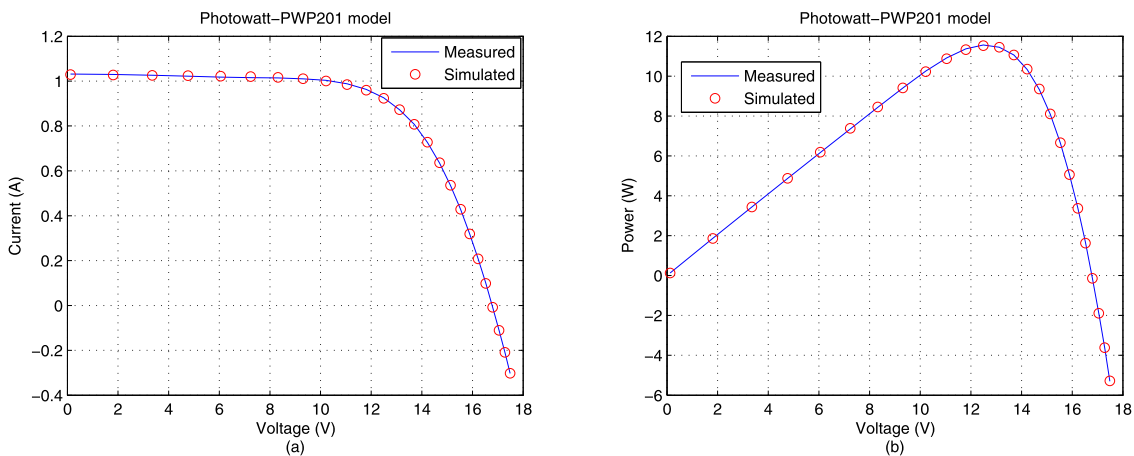


FIGURE 5. Comparison between the measured and simulated data obtained by TPTLBO for Photowatt-PWP201 module: (a) *I-V* characteristic, (b) *P-V* characteristic.

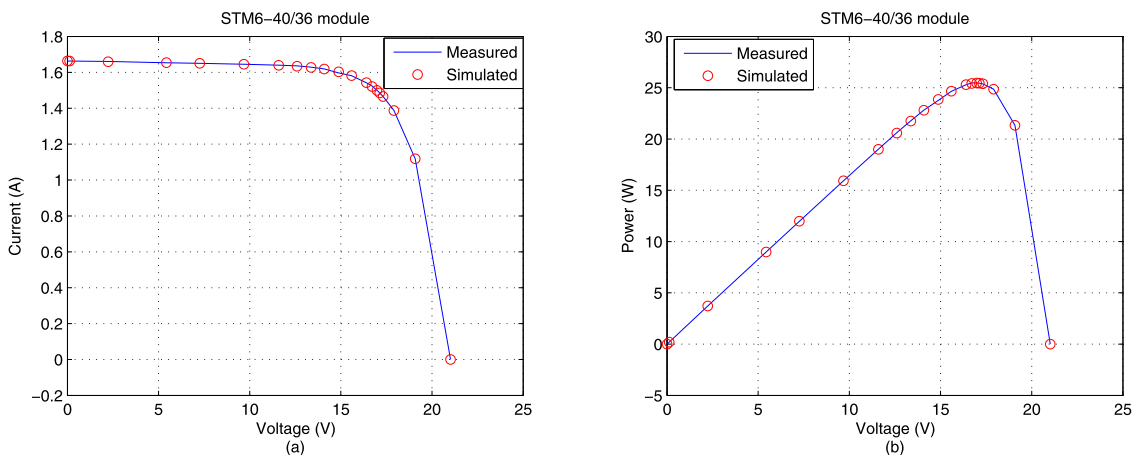


FIGURE 6. Comparison between the measured and simulated data obtained by TPTLBO for STM6-40/36 module: (a) *I-V* characteristic, (b) *P-V* characteristic.

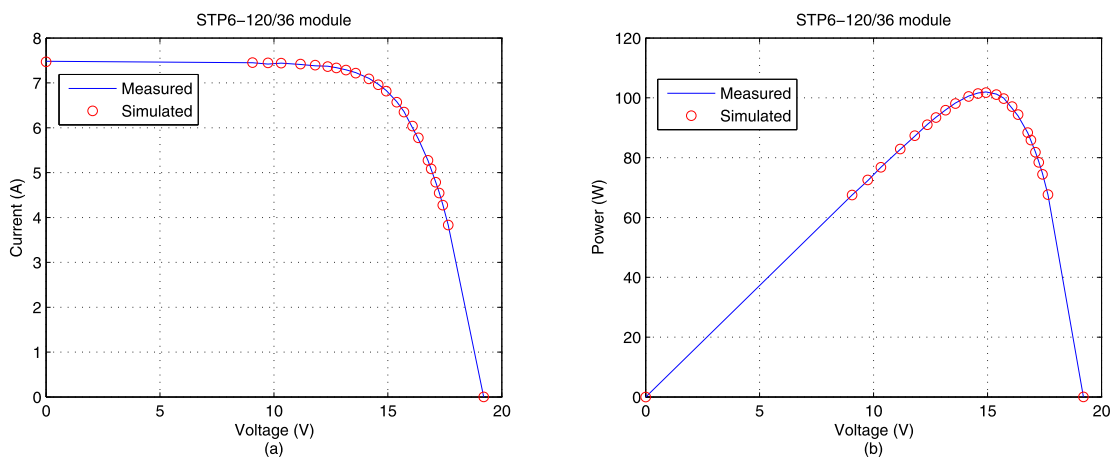


FIGURE 7. Comparison between the measured and simulated data obtained by TPTLBO for STP6-120/36 module: (a) *I-V* characteristic, (b) *P-V* characteristic.

and the measured data. In other words, the smaller IAEC, the better the extracted parameter. From Table 5, the IAEC is less than 2.0E-03, which further indicates that the measured and extracted data have a good coincidence.

C. RESULTS ON THE PV MODULES

Section V-A and V-B, the single and double diode models were employed to verify the performance of TPTLBO. In this subsection, the PV modules (Photowatt-PWP201,

TABLE 9. Simulated results of TPTLBO for Photowatt-PWP201.

Item	V (V)	$I_{measured}$ (A)	$I_{simulated}$ (A)	IAEC (A)
1	0.1248	1.0315	1.029122	0.002377909
2	1.8093	1.03	1.027384	0.002615646
3	3.3511	1.026	1.025742	0.000257862
4	4.7622	1.022	1.024104	0.002103991
5	6.0538	1.018	1.022283	0.004283411
6	7.2364	1.0155	1.019917	0.004417401
7	8.3189	1.014	1.016351	0.002350812
8	9.3097	1.01	1.010491	0.000491431
9	10.2163	1.0035	1.000679	0.002821241
10	11.0449	0.988	0.984653	0.003346651
11	11.8018	0.963	0.959697	0.003302591
12	12.4929	0.9255	0.923049	0.002451245
13	13.1231	0.8725	0.872588	0.000088159
14	13.6983	0.8075	0.80731	0.000189879
15	14.2221	0.7265	0.727958	0.001457818
16	14.6995	0.6345	0.636466	0.001966178
17	15.1346	0.5345	0.535696	0.001196071
18	15.5311	0.4275	0.428816	0.001316148
19	15.8929	0.3185	0.318669	0.000168657
20	16.2229	0.2085	0.207857	0.000642886
21	16.5241	0.101	0.098354	0.002645789
22	16.7987	-0.008	-0.00817	0.000169338
23	17.0499	-0.111	-0.11097	0.000031539
24	17.2793	-0.209	-0.20912	0.000117617
25	17.4885	-0.303	-0.30202	0.000977624
Σ	-	-	-	0.041787895

TABLE 10. Simulated results of TPTLBO for STM6-40/36.

Item	V (V)	$I_{measured}$ (A)	$I_{simulated}$ (A)	IAEC (A)
1	0	1.663	1.663458	0.000458133
2	0.118	1.663	1.663252	0.000252240
3	2.237	1.661	1.659551	0.001448804
4	5.434	1.653	1.653914	0.000914445
5	7.26	1.65	1.650566	0.000565746
6	9.68	1.645	1.64543	0.000430437
7	11.59	1.64	1.639234	0.00076595
8	12.6	1.636	1.633715	0.002284904
9	13.37	1.629	1.627288	0.001711519
10	14.09	1.619	1.618315	0.000684824
11	14.88	1.597	1.603067	0.006067380
12	15.59	1.581	1.581585	0.000584996
13	16.4	1.542	1.542327	0.000327449
14	16.71	1.524	1.521225	0.002775025
15	16.98	1.5	1.499206	0.000794279
16	17.13	1.485	1.485271	0.000271146
17	17.32	1.465	1.465643	0.000643214
18	17.91	1.388	1.387599	0.000400659
19	19.08	1.118	1.118372	0.000372103
20	21.02	0	-0.000021	0.000021314
Σ	-	-	-	0.021774563

STM6-40/36, and STP6-120/36) are chosen to further evaluate the effectiveness of our method. Tables 6-8 report the extracted results obtained from different algorithms. It can be seen that TPTLBO gains the minimum RMSE values for the three PV modules. Hence, compared with other algorithms, our method TPTLBO gives the competitive results.

Additionally, in order to verify the accuracy of the extracted parameters from TPTLBO, $I-V$ and $P-V$ curve are also respectively given in Fig. 5, 6 and 7. According to the results, the simulated data of TPTLBO are highly consistent with the measured data for Photowatt-PWP201, STM6-40/36, and STP6-120/36. Moreover, the results of IAEC is provided in Table 9-11. As can be seen from the table, IAEC values of the three different models are small, especially for Photowatt-PWP201 and STM6-40/36, so the precision of the extracted parameters is feasible.

TABLE 11. Simulated results of TPTLBO for STP6-40/36.

Item	V (V)	$I_{measured}$ (A)	$I_{simulated}$ (A)	IAEC (A)
1	0	7.48	7.470981	0.009018713
2	9.06	7.45	7.452538	0.002537554
3	9.74	7.42	7.446715	0.026714969
4	10.32	7.44	7.439092	0.000907766
5	11.17	7.41	7.420265	0.010265003
6	11.81	7.38	7.395873	0.015873147
7	12.36	7.37	7.363265	0.006735208
8	12.74	7.34	7.331483	0.008516931
9	13.16	7.29	7.28413	0.005870150
10	13.59	7.23	7.217761	0.012239401
11	14.17	7.1	7.088137	0.011862688
12	14.58	6.97	6.958449	0.011550953
13	14.93	6.83	6.81486	0.015139894
14	15.39	6.58	6.567929	0.012070635
15	15.71	6.36	6.348727	0.011272577
16	16.08	6	6.037492	0.037492386
17	16.34	5.75	5.776814	0.026813801
18	16.76	5.27	5.273765	0.003765156
19	16.9	5.07	5.081934	0.011933888
20	17.1	4.79	4.79E+00	0.004166983
21	17.25	4.56	4.546289	0.013710590
22	17.41	4.29	4.273929	0.016070931
23	17.65	3.83	3.832282	0.002282318
24	19.21	0	0.001164	0.001164343
Σ	-	-	-	0.277975972

TABLE 12. The statistical results of different PV models.

Model	Algorithm	RMSE			
		Min	Max	Mean	Std
R.T.C France solar cell (SDM)	IJAYA	9.8603E-04	1.0622E-03	9.9204E-04	1.40E-05
	PGJAYA	9.8602E-04	9.8603E-04	9.8602E-04	1.45E-09
	MLBSA	9.8602E-04	9.8602E-04	9.8602E-04	9.15E-12
	TLBO	9.8602E-04	1.2848E-03	1.0215E-03	6.95E-05
	SATLBO	9.8602E-04	9.9494E-04	9.8780E-04	2.30E-06
	LETLBO	9.8602E-04	9.8665E-04	9.8604E-03	1.14E-06
	GOTLBO	9.8602E-04	1.4388E-03	1.0289E-03	1.01E-04
	TLABC	9.8602E-04	1.0397E-03	9.9852E-04	1.86E-05
	ITLBO	9.8602E-04	9.8602E-04	9.8602E-04	2.79E-17
	TPTLBO	9.8602E-04	9.8602E-04	9.8602E-04	2.28E-17
R.T.C France solar cell (DDM)	IJAYA	9.8293E-04	1.4055E-03	1.0269E-03	9.83E-05
	PGJAYA	9.8263E-04	9.9499E-04	9.8582E-04	2.54E-06
	MLBSA	9.8249E-04	9.8798E-04	9.8518E-04	1.35E-06
	TLBO	9.8438E-04	3.0003E-03	1.1681E-03	3.77E-04
	SATLBO	9.8280E-04	1.0470E-03	9.9811E-04	1.95E-05
	LETLBO	9.8571E-04	2.4358E-03	1.0712E-03	2.76E-04
	GOTLBO	9.8407E-04	1.4380E-03	1.0453E-03	1.01E-04
	TLABC	9.8415E-04	1.5048E-03	1.0555E-03	1.55E-04
	ITLBO	9.8248E-04	9.8807E-04	9.8448E-04	1.59E-06
	TPTLBO	9.8248E-04	9.8602E-04	9.8363E-04	9.31E-07
Photowatt-PWP201 (SMM)	IJAYA	2.4251E-03	2.4393E-03	2.4289E-03	3.78E-06
	PGJAYA	2.4251E-03	2.4268E-03	2.4251E-03	3.07E-07
	MLBSA	2.4251E-03	2.4253E-03	2.4251E-03	4.34E-08
	TLBO	2.4251E-03	3.2592E-03	2.4815E-03	1.65E-04
	SATLBO	2.4251E-03	2.4291E-03	2.4254E-03	7.41E-07
	LETLBO	2.4251E-03	2.4252E-03	2.4251E-03	1.18E-08
	GOTLBO	2.4251E-03	2.4852E-03	2.4419E-03	1.38E-05
	TLABC	2.4251E-03	2.4458E-03	2.4265E-03	4.00E-06
	ITLBO	2.4251E-03	2.4251E-03	2.4251E-03	1.20E-17
	TPTLBO	2.4251E-03	2.4251E-03	2.4251E-03	1.20E-17
STM6-40/36 (SMM)	IJAYA	1.7548E-03	2.5223E-03	1.9305E-03	1.91E-04
	PGJAYA	1.7298E-03	1.7302E-03	1.7298E-03	7.82E-08
	MLBSA	1.7298E-03	1.7851E-03	1.7382E-03	1.45E-05
	TLBO	1.7950E-03	1.9866E-02	4.5368E-02	3.54E-05
	SATLBO	1.7298E-03	1.7299E-03	1.7298E-03	1.22E-08
	LETLBO	1.7298E-03	4.2554E-03	2.8158E-03	1.78E-04
	GOTLBO	1.7298E-03	1.1244E-02	4.2347E-03	6.41E-02
	TLABC	1.7298E-03	6.5053E-03	2.1827E-03	9.22E-04
	ITLBO	1.7298E-03	1.7298E-03	1.7298E-03	7.13E-18
	TPTLBO	1.7298E-03	1.7298E-03	1.7298E-03	4.96E-18
STP6-120/36 (SMM)	IJAYA	1.6731E-02	1.7304E-02	1.6891E-02	1.12E-04
	PGJAYA	1.6601E-02	1.6611E-02	1.6602E-02	2.57E-06
	MLBSA	1.6601E-02	1.8269E-02	1.6731E-02	3.01E-04
	TLBO	1.6601E-02	9.4403E-02	2.7881E-02	1.75E-02
	SATLBO	1.6601E-02	1.6601E-02	1.6601E-02	2.02E-09
	LETLBO	1.6601E-02	7.5799E-02	2.2299E-02	1.09E-02
	GOTLBO	1.6601E-02	1.8099E-01	2.9588E-02	3.05E-02
	TLABC	1.6601E-02	2.1497E-02	1.6963E-02	9.47E-04
	ITLBO	1.6601E-02	1.6601E-02	1.6601E-02	8.44E-17
	TPTLBO	1.6601E-02	1.6601E-02	1.6601E-02	7.72E-17

D. STATISTICAL RESULTS AND CONVERGENCE SPEED

Compared with nine well established in the previous sections, the superior accuracy of the extracted parameter from TPTLBO algorithm has been verified. To further prove the reliability of TPTLBO, the statistical results containing

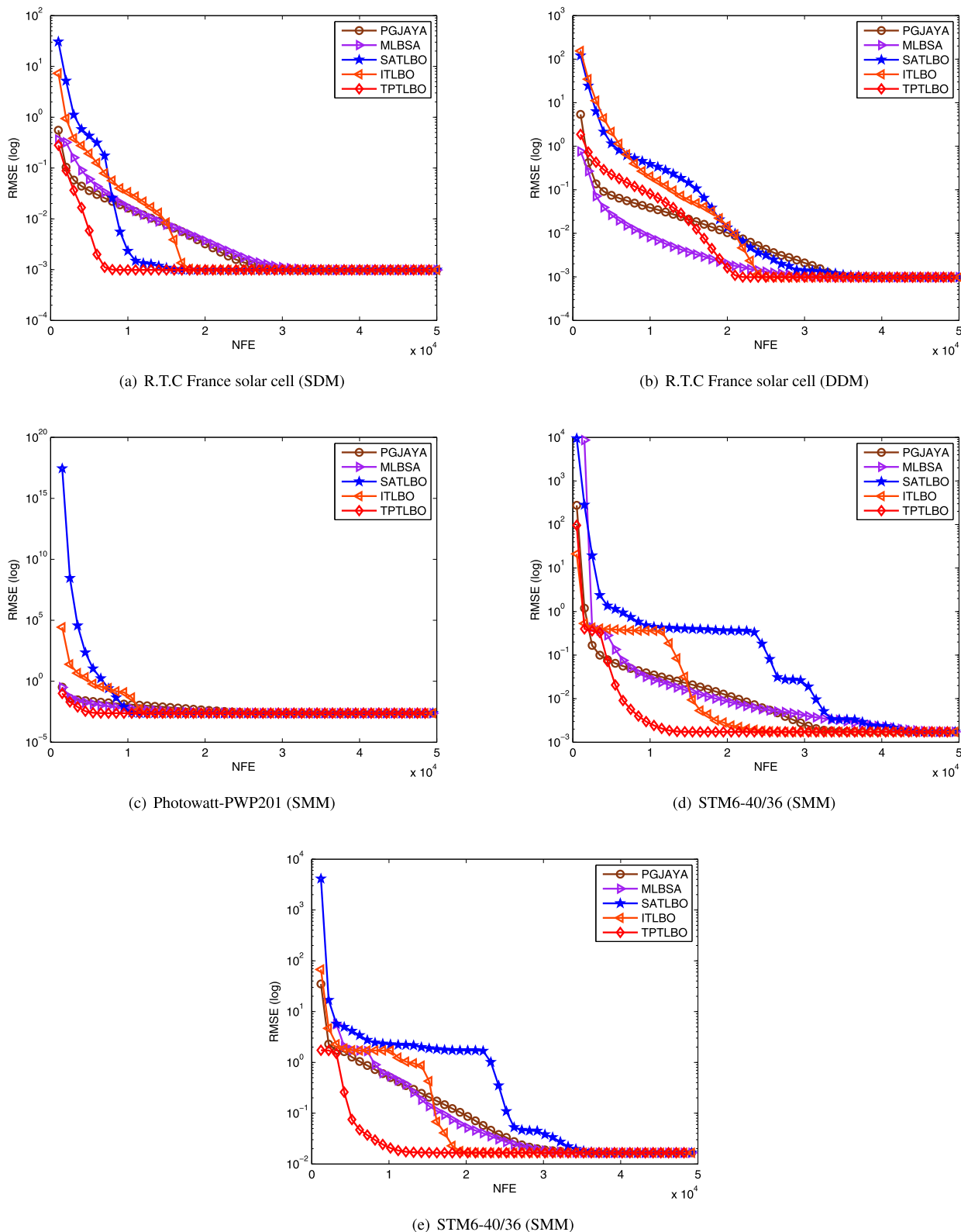


FIGURE 8. Convergence curves of different algorithms on different PV models.

minimum (Min), maximum (Max), mean value (Mean), and standard deviation (Std) are analyzed. Table 12 shows the statistical results. we can conclude follows:

- For the Min RMSE values, most algorithms can achieve the best values for SDM, STM6-40/36 and STP6-120/36 modules. In addition, all algorithms give the Min RMSE

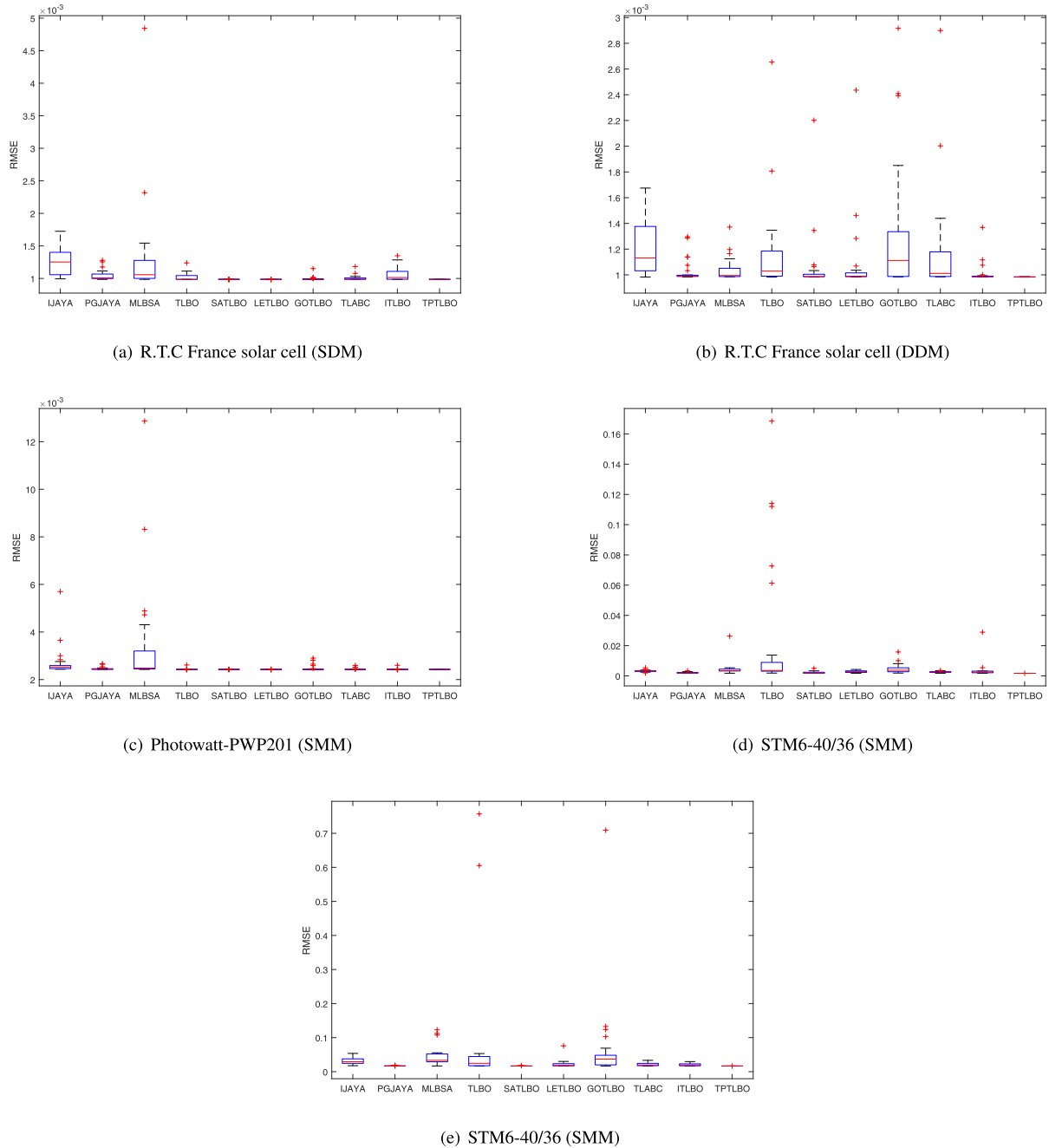


FIGURE 9. Best RMSE boxplot of different algorithm for different PV models.

TABLE 13. Comparison of TPTLBO with parameter extraction methods in literature for single diode model.

h Algorithm	I_{ph} (A)	I_d (μ A)	R_s (Ω)	R_{sh} (Ω)	α	RMSE
CPMPSO	0.7607	0.3230	0.03637	53.7185	1.4811	9.8602E-04
BLPSO	0.7608	0.3483	0.03611	53.4171	1.488	9.8615E-04
FPA	0.7608	0.3240	0.0364	53.6596	1.4815	7.7301E-04
GWO	0.7601	0.3278	0.0368	71.4883	1.4824	1.2803E-03
WDO	0.7608	0.3223	0.0367	57.7156	1.4808	8.6640E-06
TPTLBO	0.7608	0.3230	0.0364	53.7185	1.4812	9.8602E-04

value for Photowatt-PWP201, whereas only TPTLBO and ITLBO obtain the best results for DDM.

- With respect to the Max and Mean RMSE values, it is obvious that TPTLBO shows significant performance in

all models compared with other algorithms, particularly DDM. Additionally, ITLBO, SATLBO, MLBSA, and PGJAYA also obtain relatively good results.

- In terms of the Std values, it can be seen that TPTLBO has provided the best results, followed by ITLBO. Hence, TPTLBO and ITLBO show a preferable robustness.

According to the above analysis, four algorithms (ITLBO, SATLBO, MLBSA and PG-JAYA) also provide competitive results compared to TPTLBO. To this end, Fig. 8 shows the convergence graphs of different algorithms on different

TABLE 14. Comparison of TPTLBO with parameter extraction methods in literature for double diode model.

Algorithm	I_{ph} (A)	I_{d1} (μ A)	R_s (Ω)	R_{sh} (Ω)	a_1	I_{d2} (μ A)	a_2	RMSE
CPMPSO	0.7607	0.7493	0.0367	55.4854	2.0000	0.2259	1.4510	9.8248E-04
BLPSO	0.7601	0.1488	0.0359	63.4574	1.8066	0.3256	1.4852	1.0822E-03
FPA	0.7607	0.3008	0.0363	52.3475	1.4777	0.1661	2.0000	7.8425E-04
GWO	0.7609	0.5099	0.0370	56.8758	1.9140	0.2161	1.4472	1.0274E-03
WDO	0.7606	0.2531	0.0374	52.6608	1.5116	0.0482	1.3843	6.5237E-06
TPTLBO	0.7608	0.7434	0.0367	55.4831	2.0000	0.2266	1.4513	9.8248E-04

TABLE 15. Comparison of TPTLBO with parameter extraction methods in literature for Photowatt-PWP201 module.

Algorithm	I_{ph} (A)	I_d (μ A)	R_s (Ω)	R_{sh} (Ω)	a	RMSE
CPMPSO	1.0305	3.4823	1.2012	981.9823	48.6428	2.4251E-03
BLPSO	1.0304	3.4854	1.2013	986.6686	48.6460	2.4251E-03
FPA	1.0305	3.4821	1.2013	981.8646	48.6427	2.0546E-03
GWO	1.0298	4.3863	1.1757	1186.606	49.5469	2.5261E-03
WDO	1.0295	4.0585	1.1733	973.1520	49.2487	2.7960E-03
TPTLBO	1.0305	3.4823	1.2013	981.9822	48.6428	2.4251E-03

TABLE 16. Comparison of TPTLBO with parameter extraction methods in literature for STM6-40/36 module.

Algorithm	I_{ph} (A)	I_d (μ A)	R_s (Ω)	R_{sh} (Ω)	a	RMSE
CPMPSO	1.6639	1.7387	0.0042	15.9282	1.5203	1.7298E-03
BLPSO	1.6602	6.3076	1.07E-08	30.7045	1.6763	3.5960E-03
FPA	1.6610	4.7541	0.0007	23.0258	1.6395	3.0632E-03
GWO	1.6566	6.9194	0.0001	62.9688	1.6885	4.3409E-03
WDO	1.6561	16.615	0	445.904	1.8184	1.6278E-02
TPTLBO	1.6639	1.7387	0.0043	15.9283	1.5203	1.7298E-03

TABLE 17. Comparison of TPTLBO with parameter extraction methods in literature for STP6-120/36 module.

Algorithm	I_{ph} (A)	I_d (μ A)	R_s (Ω)	R_{sh} (Ω)	a	RMSE
CPMPSO	7.4725	2.3350	0.0045	22.2199	1.2601	1.6601E-02
BLPSO	7.5141	9.8195	0.0038	642.9095	1.3926	3.1839E-02
FPA	7.4639	3.6881	0.0044	1416.9000	1.2997	1.8422E-02
GWO	7.4606	2.4467	0.0046	201.9213	1.2640	1.6844E-02
WDO	7.4107	50.000	0.0018	1197.000	1.5815	1.1132E-01
TPTLBO	7.4725	2.3350	0.0046	22.2199	1.2601	1.6601E-02

models, and we will further analyzes the performance of the algorithm. It is obvious that TPTLBO shows the fastest convergence rate, especially for SDM, STM6-40/36 and STP6-120/36 modules. Therefore, the proposed TPTLBO algorithm can provide accurate and reliable parameter values faster than other comparison algorithms.

In addition, to show the distribution results obtained from different algorithms, the boxplot of different PV models is given in Fig. 9. It can be seen that TPTLBO demonstrates the superior performance in terms of accuracy and robustness.

It's worth noting that the results obtained by TPTLBO and ITLBO are similar/close from Table 6-8 and Table 12. However, it can be seen from Fig. 8 that TPTLBO converges faster than ITLBO. Additionally, in Fig. 9, our algorithm shows better robustness. Therefore, compared with ITLBO, TPTLBO is better in both convergence and robustness.

E. COMPARISON WITH RESULTS IN THE LITERATURE

In this subsection, TPTLBO is compared with other methods that were used in parameter extraction, including CPMPSO [35], BLPSO [36], flower pollination algorithm (FPA) [37], grey wolf optimizer (GWO) [38], and wind driven

TABLE 18. Optimal parameters extracted by TPTLBO for two types of PV modules at different irradiance and temperature of 25 °C.

Parameter	Mono-crystalline SM55	Multi-crystalline KC200GT
$G = 200 W/m^2$		
I_{ph} (A)	0.69150983	1.64615448
I_o (μ A)	0.14641172	0.00052100
R_s (Ω)	0.00796166	0.00705762
R_{sh} (Ω)	12.45029748	12.78049260
a	1.38066049	1.00324346
RMSE	3.2069E-04	1.4185E-03
$G = 400 W/m^2$		
I_{ph} (A)	1.38284413	3.28784893
I_o (μ A)	0.10041951	0.00148987
R_s (Ω)	0.01101817	0.00654775
R_{sh} (Ω)	11.86251222	13.92758141
a	1.35198818	1.05503876
RMSE	7.0761E-04	1.4262E-03
$G = 600 W/m^2$		
I_{ph} (A)	2.07089654	4.93430794
I_o (μ A)	0.15551374	0.00386144
R_s (Ω)	0.00918063	0.00624700
R_{sh} (Ω)	12.50190379	13.75928956
a	1.38753423	1.10402054
RMSE	8.2395E-04	1.2977E-03
$G = 800 W/m^2$		
I_{ph} (A)	2.76038170	6.57132737
I_o (μ A)	0.14395059	0.00095306
R_s (Ω)	0.00937751	0.00661732
R_{sh} (Ω)	12.77440241	13.76894813
a	1.38114451	1.03531971
RMSE	6.6858E-04	1.6310E-03
$G = 1000 W/m^2$		
I_{ph} (A)	3.45010356	8.21689146
I_o (μ A)	0.17115392	0.00226316
R_s (Ω)	0.00914299	0.00636448
R_{sh} (Ω)	13.44167955	14.25944454
a	1.39575286	1.07686676
RMSE	1.1462E-03	1.5421E-03

optimization (WDO) [39]. ³ The parameters of these algorithms are expressed in Table 1.

For the single diode model, the experimental results are shown in Table 13. It can be seen that WDO get the best RMSE (8.6640E-06), followed by FPA (7.7301E-04), TPTLBO (9.8602E-04),CPMPSO (9.8602E-04), BLPSO (1.0312E-03), and GWO (1.2210E-03).

For the double diode model, Table 14 gives the results obtained from different algorithm. For this model, WDO get the best RMSE (6.5237E-06). They are better than BLPSO, FPA, TPTLBO, CPMPSO and GWO.

For the PV module model (Photowatt-PWP201, STM6-40/36, and STP6-120/36), Tables 15-17 present the extracted results obtained from CPMPSO, BLPSO, FPA,

³It is worth noting that the FPA result in Table 13-15 were obtain from [37], and the FPA results in Table 16-17 were obtained from [35]. Similarly, WDO results in Table 13-14 were obtained from [40], and the WDO results in Table 15-17 were obtained from [35]. The results of other methods were derived from [35].

TABLE 19. Optimal parameters extracted by TPTLBO for two types of PV modules at different temperature and irradiance of 1000 W/m^2 .

PV module	Temperature	I_{ph} (A)	I_o (μA)	R_s (Ω)	R_{sh} (Ω)	a	RMSE
Mono-crystalline SM55	25 °C	3.45010356	0.17115392	0.00914299	13.44167979	1.39575286	1.1462E-03
	40 °C	3.46913752	1.14510976	0.00869711	14.80747794	1.41783976	3.7888E-03
	60 °C	3.49460847	6.90949935	0.00885294	13.46899847	1.40514174	3.7804E-03
Multi-crystalline KC200GT	25 °C	8.21689146	0.00224195	0.00636693	14.13954085	1.07641029	1.5390E-03
	50 °C	8.29530520	0.12595295	0.00621583	17.66462868	1.11729226	2.7465E-03
	75 °C	8.37766296	1.63082275	0.00634255	14.63996983	1.10147993	4.4729E-03

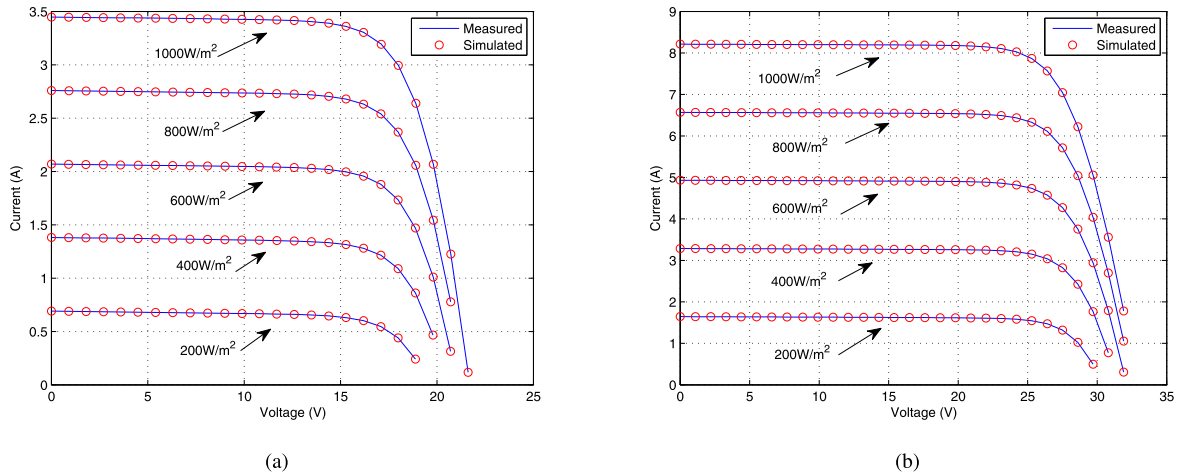


FIGURE 10. Comparison between the measured and simulated data obtained by TPTLBO at different irradiance and temperature of 25 °C: (a) Mono-crystalline SM55, (b) Multi-crystalline KC200GT.

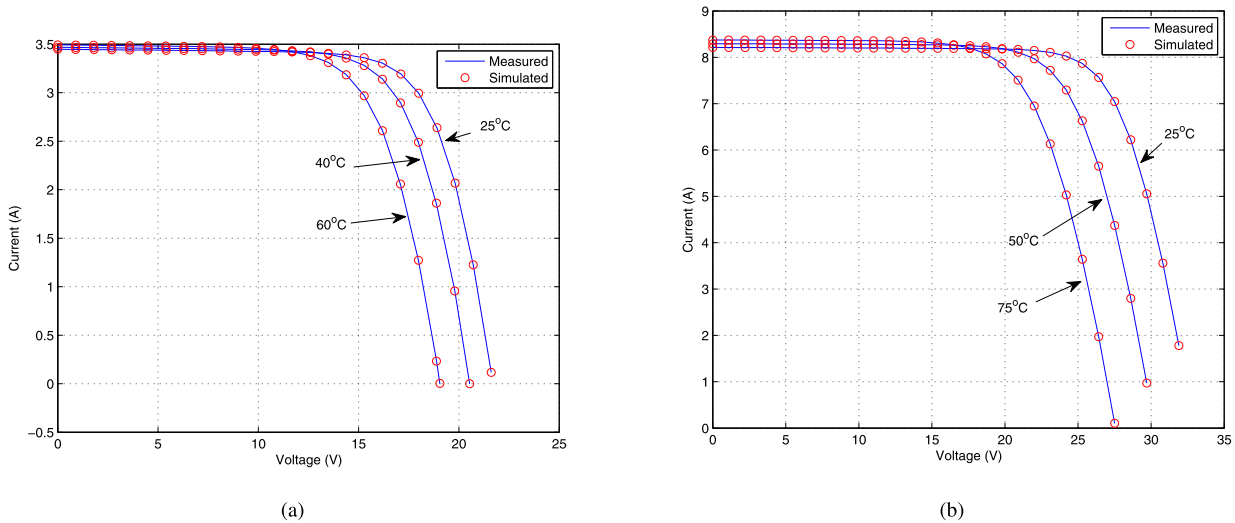


FIGURE 11. Comparison between the measured and simulated data obtained by TPTLBO at different temperature and irradiance of 1000 W/m^2 : (a) Mono-crystalline SM55, (b) Multi-crystalline KC200GT.

GWO, WDO, TPTLBO. From the results, it can be seen that TPTLBO and CPMPOS obtain the best RMSE in STM6-40/36 and STP6-120/36 whereas FPA got the best RMSE in Photowatt-PWP201.

Based on the above comparisons, it illustrates that TPTLBO can obtain similar or better results compared with these approaches; thus, it can be considered as an efficient alternative method for parameter extraction problems in different PV models. Note that FPA and WDO show better

results in single/double diode model and Photowatt-PWP201, which will motivate us to apply several ideas of these two methods to improve the efficiency of the algorithm in the future.

F. RESULTS ON EXPERIMENTAL DATA FROM THE MANUFACTURERS DATA SHEET

To further verify the reliability of TPTLBO, two practice PV module models (Multi-crystalline KC200GT and

Mono-crystalline SM55) [15] are selected as test sets. Their experimental data are obtained by extracting the I-V curves given in the manufacturers data sheet at different five irradiance and three temperature conditions.

The range of parameters are set as $I_{ph} \in [0, 2I_S]$ (A), $I_o \in [0, 100]$ (μA), $R_s \in [0, 2]$ (Ω), $R_{sh} \in [0, 5000]$ (Ω), and $a \in [1, 4]$. I_S is short-circuit current under non-standard conditions related to irradiance (G) and temperature (T), which is expressed as follows:

$$I_S(G, T) = I_{S_STC} \cdot \frac{G}{G_{STC}} + \alpha \cdot (T - T_{STC}) \quad (24)$$

where I_{S_STC} , G_{STC} , and T_{STC} are the short circuit current, irradiance, and temperature at standard test conditions, respectively. α is the temperature coefficient for short circuit current at standard test conditions.

The best parameters extracted by TPTLBO at different irradiance and temperature are given in Table 18 and 19, respectively. Moreover, Fig. 10 and 11 give the comparisons between the simulated and measured data of the two PV module models at different irradiance and temperature.

From Table 18, it is clear that I_{ph} increases gradually while the other four parameters (I_o , R_s , R_{sh} , and a) fluctuate slightly with the increase of irradiance. From Table 19, it is obvious that I_{ph} increases gradually while I_o , R_s , R_{sh} , and a fluctuate slightly as the temperature increases. In addition, with respect to the I-V curve of the two PV module models given in Fig. 10 and 11, the simulated data agree well with the measured data at different five irradiance and three temperature conditions. It is worth noting that TPTLBO also obtained accurate parameters at low irradiance, which makes sense for maximum power point tracking (MPPT) of PV systems. Since several modules in the PV system suffer from certain mismatches, such as partial shading.

VI. CONCLUSION

In this paper, a triple-phase teaching-learning-based optimization algorithm (TPTLBO) is presented to accurately and reliably extract the unknown parameters of different PV models. In TPTLBO, a buffer phase is introduced in teaching and learning phase to further balance the exploration and exploitation by adopting a centroid strategy. In addition, a dynamic control technique is developed to control the amount of knowledge acquired from other learners and improve the search efficiency of the algorithm. TPTLBO is verified through parameters extraction problems of single diode, double diode, and PV module models. Experiment results demonstrate that TPTLBO obtains the superior performance when compared with other state-of-the-art algorithm. Hence, TPTLBO can be considered as a feasible alternative for parameter extraction of other complex PV models. In future, TPTLBO will be used to deal with the maximum power point tracking problem in photovoltaic systems and other energy problem and economic dispatch problem in power systems.

REFERENCES

- [1] M. A. Awadallah, "Variations of the bacterial foraging algorithm for the extraction of PV module parameters from nameplate data," *Energy Convers. Manage.*, vol. 113, pp. 312–320, Apr. 2016.
- [2] M. F. AlHajri, K. M. El-Naggar, M. R. AlRashidi, and A. K. Al-Othman, "Optimal extraction of solar cell parameters using pattern search," *Renew. Energy*, vol. 44, pp. 238–245, Aug. 2012.
- [3] S. Xu and Y. Wang, "Parameter estimation of photovoltaic modules using a hybrid flower pollination algorithm," *Energy Convers. Manage.*, vol. 144, pp. 53–68, Jul. 2017.
- [4] L. El Chaar, L. A. Lamont, and N. El Zein, "Review of photovoltaic technologies," *Renew. Sustain. Energy Rev.*, vol. 15, pp. 2165–2175, Jun. 2011.
- [5] V. Lo Brano and G. Ciulla, "An efficient analytical approach for obtaining a five parameters model of photovoltaic modules using only reference data," *Appl. Energy*, vol. 111, pp. 894–903, Nov. 2013.
- [6] K. Yu, J. J. Liang, B. Y. Qu, X. Chen, and H. Wang, "Parameters identification of photovoltaic models using an improved JAYA optimization algorithm," *Energy Convers. Manage.*, vol. 150, pp. 742–753, Oct. 2017.
- [7] A. Askarzadeh and A. Rezaadeh, "Parameter identification for solar cell models using harmony search-based algorithms," *Sol. Energy*, vol. 86, no. 11, pp. 3241–3249, Nov. 2012.
- [8] T. Easwarakhanthan, J. Bottin, I. Bouhouch, and C. Boutrif, "Nonlinear minimization algorithm for determining the solar cell parameters with microcomputers," *Int. J. Sol. Energy*, vol. 4, no. 1, pp. 1–12, Jan. 1986.
- [9] N. Thanh Tong, K. Kamolpattana, and W. Pora, "A deterministic method for searching the maximum power point of a PV panel," in *Proc. 12th Int. Conf. Electr. Eng./Electron., Comput., Telecommun. Inf. Technol. (ECTI-CON)*, Jun. 2015, pp. 1–6.
- [10] X. Chen, B. Xu, C. Mei, Y. Ding, and K. Li, "Teaching-learning-based artificial bee colony for solar photovoltaic parameter estimation," *Appl. Energy*, vol. 212, pp. 1578–1588, Feb. 2018.
- [11] M. Zagrouba, A. Sellami, M. Bouaicha, and M. Ksouri, "Identification of PV solar cells and modules parameters using the genetic algorithms: Application to maximum power extraction," *Sol. Energy*, vol. 84, no. 5, pp. 860–866, May 2010.
- [12] H. Wei, J. Cong, X. Lingyun, and S. Deyun, "Extracting solar cell model parameters based on chaos particle swarm algorithm," in *Proc. Int. Conf. Electric Inf. Control Eng.*, Apr. 2011, pp. 398–402.
- [13] W. Gong and Z. Cai, "Parameter extraction of solar cell models using repaired adaptive differential evolution," *Sol. Energy*, vol. 94, pp. 209–220, Aug. 2013.
- [14] S. Li, W. Gong, X. Yan, C. Hu, D. Bai, and L. Wang, "Parameter estimation of photovoltaic models with memetic adaptive differential evolution," *Sol. Energy*, vol. 190, pp. 465–474, Sep. 2019.
- [15] S. Li, Q. Gu, W. Gong, and B. Ning, "An enhanced adaptive differential evolution algorithm for parameter extraction of photovoltaic models," *Energy Convers. Manage.*, vol. 205, Feb. 2020, Art. no. 112443.
- [16] Z. Wu, D. Yu, and X. Kang, "Parameter identification of photovoltaic cell model based on improved ant lion optimizer," *Energy Convers. Manage.*, vol. 151, pp. 107–115, Nov. 2017.
- [17] K. M. El-Naggar, M. R. AlRashidi, M. F. AlHajri, and A. K. Al-Othman, "Simulated annealing algorithm for photovoltaic parameters identification," *Sol. Energy*, vol. 86, no. 1, pp. 266–274, Jan. 2012.
- [18] D. Oliva, E. Cuevas, and G. Pajares, "Parameter identification of solar cells using artificial bee colony optimization," *Energy*, vol. 72, pp. 93–102, Aug. 2014.
- [19] J. P. Ram, T. S. Babu, T. Dragicicvic, and N. Rajasekar, "A new hybrid bee pollinator flower pollination algorithm for solar PV parameter estimation," *Energy Convers. Manage.*, vol. 135, pp. 463–476, Mar. 2017.
- [20] Q. Niu, L. Zhang, and K. Li, "A biogeography-based optimization algorithm with mutation strategies for model parameter estimation of solar and fuel cells," *Energy Convers. Manage.*, vol. 86, pp. 1173–1185, Oct. 2014.
- [21] X. Yuan, Y. Xiang, and Y. He, "Parameter extraction of solar cell models using mutative-scale parallel chaos optimization algorithm," *Sol. Energy*, vol. 108, pp. 238–251, Oct. 2014.
- [22] A. Fathy and H. Rezk, "Parameter estimation of photovoltaic system using imperialist competitive algorithm," *Renew. Energy*, vol. 111, pp. 307–320, Oct. 2017.
- [23] R. V. Rao, V. J. Savsani, and D. P. Vakharia, "Teaching-learning-based optimization: An optimization method for continuous non-linear large scale problems," *Inf. Sci.*, vol. 183, no. 1, pp. 1–15, Jan. 2012.
- [24] F. Zou, L. Wang, X. Hei, and D. Chen, "Teaching-learning-based optimization with learning experience of other learners and its application," *Appl. Soft Comput.*, vol. 37, pp. 725–736, Dec. 2015.

- [25] Z. Chen, L. Wu, P. Lin, Y. Wu, and S. Cheng, "Parameters identification of photovoltaic models using hybrid adaptive Nelder-Mead simplex algorithm based on eagle strategy," *Appl. Energy*, vol. 182, pp. 47–57, Nov. 2016.
- [26] K. Yu, X. Chen, X. Wang, and Z. Wang, "Parameters identification of photovoltaic models using self-adaptive teaching-learning-based optimization," *Energy Convers. Manage.*, vol. 145, pp. 233–246, Aug. 2017.
- [27] S. Li, W. Gong, X. Yan, C. Hu, D. Bai, L. Wang, and L. Gao, "Parameter extraction of photovoltaic models using an improved teaching-learning-based optimization," *Energy Convers. Manage.*, vol. 186, pp. 293–305, Apr. 2019.
- [28] R. V. Rao, V. J. Savsani, and D. P. Vakharia, "Teaching-learning-based optimization: A novel method for constrained mechanical design optimization problems," *Comput.-Aided Des.*, vol. 43, no. 3, pp. 303–315, Mar. 2011.
- [29] M. Črepinšek, S.-H. Liu, and L. Mernik, "A note on teaching-learning-based optimization algorithm," *Inf. Sci.*, vol. 212, pp. 79–93, Dec. 2012.
- [30] X.-G. Zhou and G.-J. Zhang, "Abstract convex underestimation assisted multistage differential evolution," *IEEE Trans. Cybern.*, vol. 47, no. 9, pp. 2730–2741, Sep. 2017.
- [31] Z. Liao, W. Gong, X. Yan, L. Wang, and C. Hu, "Solving nonlinear equations system with dynamic repulsion-based evolutionary algorithms," *IEEE Trans. Syst., Man, Cybern., Syst.*, vol. 50, no. 4, pp. 1590–1601, Apr. 2020.
- [32] N. T. Tong and W. Pora, "A parameter extraction technique exploiting intrinsic properties of solar cells," *Appl. Energy*, vol. 176, pp. 104–115, Aug. 2016.
- [33] K. Yu, B. Qu, C. Yue, S. Ge, X. Chen, and J. Liang, "A performance-guided JAYA algorithm for parameters identification of photovoltaic cell and module," *Appl. Energy*, vol. 237, pp. 241–257, Mar. 2019.
- [34] W. Shao, D. Pi, and Z. Shao, "A hybrid discrete optimization algorithm based on teaching-probabilistic learning mechanism for no-wait flow shop scheduling," *Knowl.-Based Syst.*, vol. 107, pp. 219–234, Sep. 2016.
- [35] J. Liang, S. Ge, B. Qu, K. Yu, F. Liu, H. Yang, P. Wei, and Z. Li, "Classified perturbation mutation based particle swarm optimization algorithm for parameters extraction of photovoltaic models," *Energy Convers. Manage.*, vol. 203, Jan. 2020, Art. no. 112138.
- [36] X. Chen, H. Tianfield, C. Mei, W. Du, and G. Liu, "Biogeography-based learning particle swarm optimization," *Soft Comput.*, vol. 21, no. 24, pp. 7519–7541, Dec. 2017.
- [37] D. F. Alam, D. A. Yousri, and M. B. Eteiba, "Flower pollination algorithm based solar PV parameter estimation," *Energy Convers. Manage.*, vol. 101, pp. 410–422, Sep. 2015.
- [38] S. Mirjalili, S. M. Mirjalili, and A. Lewis, "Grey wolf optimizer," *Adv. Eng. Softw.*, vol. 69, pp. 46–61, Mar. 2014.
- [39] Z. Bayraktar, M. Komurcu, J. A. Bossard, and D. H. Werner, "The wind driven optimization technique and its application in electromagnetics," *IEEE Trans. Antennas Propag.*, vol. 61, no. 5, pp. 2745–2757, May 2013.
- [40] M. Derick, C. Rani, M. Rajesh, M. E. Farrag, Y. Wang, and K. Busawon, "An improved optimization technique for estimation of solar photovoltaic parameters," *Sol. Energy*, vol. 157, pp. 116–124, Nov. 2017.



ZUOWEN LIAO received the B.Sc. and M.Sc. degrees in computer science from the Wuhan Institute of Chemical Technology, Wuhan, China, in 2006 and 2010, respectively. He is currently pursuing the Ph.D. degree in computer science with the China University of Geosciences, Wuhan.

His current research interests include evolutionary computation, memetic computation, and computational intelligence.



ZHIKUN CHEN received the B.Sc. degree from Nanning Normal University, Nanning, China, in 2003, and the M.Sc. and Ph.D. degrees from the China University of Geosciences, Wuhan, in 2008 and 2018, respectively. He is currently an Associate Professor with the Guangxi Key Laboratory of Marine Disaster in the Beibu Gulf, College of Resources and Environment, Beibu Gulf University, Qinzhou, China.



SHUIJIA LI received the B.Sc. degree from the Hubei University of Arts and Science, Xiangyang, China, in 2017. He is currently pursuing the Ph.D. degree in computer science with the China University of Geosciences, Wuhan, China.

His current research interests include evolutionary computation, computational intelligence and its application.

• • •